



Chemical and Electrochemical Investigation of a Novel Liquid Crystal as an Anticorrosion Agent for Mild Steel in Acidic Media

Ahmed M. El-Sawy, Hazem F. Khalil, Ashraf M. Ashmawy *

Chemistry Department, Faculty of Science (boys), Al-Azhar University, 11884, (EGYPT).



CrossMark

Abstract

In this work, inhibitory behaviour of the new azomethan compound (I-N-C8) was studied by electrochemical potentiodynamic polarization (PDP), impedance spectroscopy (EIS), and electrochemical frequency modulation (EFM), mass loss measurement, and UV-Visible spectroscopy. The structure was determined by Fourier transform infrared spectroscopy FTIR and mass spectrometry. Also the thermotropic behaviour of the studied liquid-crystal was determined by differential scanning calorimetry (DSC). The results showed that, the prepared compound revealed liquid-crystalline properties and high inhibition efficiency of about 96 %. These results make it more preferred than other inhibitors, in addition to the low cost, more availability of raw material and reduction of pollution.

Keywords: corrosion inhibitor; Mild steel; liquid crystal; differential scanning calorimetry

1. Introduction

Mild steel (MS) has a wide range of industrial and machinery applications in the Arab Republic of Egypt, such as buildings, packaging, and pipeline manufacturing, due to its special mechanical properties, high availability, and low price. In spite of these advantages, MS has a disadvantage when immersed in an aggressive medium, such as acid, where corrosion occurs [1]. Because MS is susceptible to corrosion, it is inappropriate for use in an acid environment. For example, in MS steam boilers, the formation of scale is a common occurrence. In order to remove this scale, the boiler surface has to treat by hydrochloric acid. To avoid the loss of metal during this process, the addition of corrosion inhibitor is required [2]. The corrosion of metals, which remains a global scientific problem, has had a negative effect on the metallurgical engineering, petroleum, and chemical industries [3]. According to research performed by NACE (National Association of Corrosion Engineers) International, the annual global cost of corrosion is \$2.5 trillion, which is estimated approximately 3.4 % of the world's GDP (gross

domestic product). In case of using corrosion inhibitor, it is possible to avoid losses of metal during this process, the addition of corrosion inhibitor is required [2]. The corrosion of metals, which remains a global scientific problem, has had a negative effect on the metallurgical engineering, petroleum, and chemical industries [3]. According to research performed by NACE (National Association of Corrosion Engineers) International, the annual global cost of corrosion is \$2.5 trillion, which is estimated approximately 3.4 % of the world's GDP (gross domestic product). In case of using corrosion inhibitor, it is possible to avoid losses between 15 and 35% of that cost, or 375–\$875 billion [4]. Corrosion inhibitors are chemical compounds that are used to control metal corrosion in different environments.

Organic compounds containing electronegative function groups, such as N, S, and O atoms, in addition to π electrons in triple or conjugated double bonds, are usually used as inhibitors [5, 6]. Inhibitors delay the rate of corrosion by protecting or covering the metal surface from direct contact with acidic media. Organic inhibitors primarily function by forming a film on the

*Corresponding author e-mail: ashraf_ashmawy2002@azhar.edu.eg; (Ashraf Mahmoud Ashmawy).

Receive Date: 01 June 2022, **Accept Date:** 14 October 2022, **First Publish Date:** 14 October 2022

DOI: 10.21608/EJCHEM.2022.142387.6224

©2022 National Information and Documentation Center (NIDOC)

metal surface, covering the active centres from direct exposure to the acidic medium, there by isolating the oxidation-reduction reactions occurring on the metal surface, and this phenomenon is known as adsorption[7]. Chemical compounds inhibit corrosion by chemisorbing at the metal/solution interface, forming a protective layer that prevents corrosion on the metal's surface. The effect of a corrosion inhibitor depends on the adsorption quality of the surface metal, which changes according to its nature and charge; also, factors such as the nature, class of the corrosive solution, as well as the inhibitor's structure, affect the inhibition efficiency [8]. The sizes of donor atoms, their electron densities, and the orbital shapes of the donating electrons in organic molecules all influence adsorption quality [9, 10].

Liquid crystals LCs can be defined as a state of matter that exists between crystalline solids and isotropic liquids, combining their properties [11]. There are many general parameters associated with LCs materials. Molecular structure with a long axis rod and a strong dipole and/or easily polarizable substituents and aliphatic chain which has motion properties [12, 13]. The structure of organic compounds is closely related to and dependent on their liquid-crystalline behaviour. Halogen groups showed a strong influence on the LCs properties when they occupied the terminal position in the molecular structure [14]. The iodine atoms enlarge the molecular polarizability and led to higher mesophase stability. [15]. This work aims to prepare a new organic inhibitor that includes the above mentioned groups and also shows LCs properties and then investigates its anticorrosion properties for MS in 1 M HCl solution at various temperatures. On the other hand, the availability and cost of the starting materials have been considered side by side with the produced inhibition efficiency. Regarding corrosion efficiency, table 1 shows a comparison between the prepared compound and many of published related inhibitors. Four different compounds were prepared in Ref.40, among them this compound showed the highest η %.

2. Experimental:

2.1. Materials and Methods

4-(dimethyl amino) benzaldehyde 98%), (1-bromooctan 98%), and (4-iodoaniline) were supplied by Alfa Aesar Co. Ethanol absolute (HPLC grade) was supplied by Sigma-Aldrich Co. and used directly. The chemical composition of the used MS is as follows, (wt. %): 0.093 % C, 0.011 % Si, 0.853% Mn, 0.014%

P, 0.013% Ni, 0.025 % Cr, 0.032% Al and the rest Fe.

2.2. Preparation of The Inhibitor (I-N-C8)

Novel inhibitor was synthesized in two steps. In the first step, a molar ratio of (1:1) 4-(dimethylamino) benzaldehyde (3.73gm) and 1-bromooctan (4.82 gm) was heated for 12 h under reflux in 250 ml of absolute ethanol. Then the reaction mixture was cooled to room temperature and purified. In the second step, a condensation reaction between 4-formyl-N,N-dimethyl-N-octylbenzenaminium bromide (4.28 gm) and 4-iodoaniline (2.74 gm) in the molar ratio of (1:1) was performed for 12 h under reflux in 250 ml ethanol. After that, the product was recrystallized from ethanol to produce I-N-C8[16, 17].

2.3. Characterization of Inhibitor

Chemical structure of the new compound was investigated using infrared (IR) spectroscopy with a Nicolet iS10 spectrometer and mass spectroscopy with a Shimadzu GC/MSQP5050A spectrometer. The mesosphere behaviour was investigated by DSC with the conditions that nitrogen must be a pure gas, heating and cooling rates of 10 °C/min., and a sample mass of 2–3 mg.

2.4. Electrochemical Methods for Evaluation Novel Compound as Corrosion Inhibitor

The (PDP) Potentiodynamic polarization method was performed by a Gamry Reference 3000 Potentiostat/Galvanostat/ZRA. Electrochemical test methods were performed on a three-electrode cell containing a counter electrode (platinum wire), a reference electrode (saturated calomel), and a working electrode (MS sample). The dimensions of the working electrode were adjusted to be; 2 cm × 1 cm × 0.4 cm. The surface of the MS samples were scraped with emery paper (grade 600, 800, and 1200), then cleaned with distilled water, acetone, and finally air-dried at 298 K, the working electrode was immersed in 50 ml of (1 M HCl) solution with and without various concentrations of I-N-C8 compound (50 to 0.5×10^{-5} M) for 30 min. The PDP test was performed at a scan rate of 5 mV s⁻¹, and EIS test was performed after immersing of the electrode in a 1 M HCl solution for 1 h at 10 mV and over a frequency range of 100 to 200 mHz at 298 K. EFM was performed at 10 mV amplitude AC voltage with two frequencies of 2 and 5 Hz[18, 19].

2.5. Chemical Method for Evaluation of The New Compound as Corrosion Inhibitor

The gravimetric method was used to calculate the corrosion rate of MS in 1 M HCl solution for 24 hours at five different temperatures: 298, 308, 318, 328, and 338 K. The MS samples have the same composition and dimensions as previously described for electrochemical tests. The tested samples were prepared as above, weighed, and then immersed for 24 hours in 1 M HCl. After 24 hrs of immersion, the sample slides were removed from the solution, dried, and reweighed. The difference in weight (ΔW) is calculated by the following equation:

$$\Delta W = WB - WA \quad (1)$$

Where WB and WA are the weight of the sample before and after immersion in the test solution respectively, ΔW calculated in grams.

The corrosion rate can be calculated as follows:

$$C.R = \Delta W \times K \div (A \times t \times d) \quad (2)$$

Where C.R is the corrosion rate in mm/year, A is the surface area of the metal sample in cm^2 , t is the immersion time in hours, d is the density of the metal in g/cm^3 , and K is corrosion constant = 8.75×10^4 . Corrosion rate and weight loss (% IE) were used to determine the inhibition efficiency (% IE) and degree of surface coverage (θ) of I-N-C8 was by following equation [20]:

$$\theta = 1 - (C.R \text{ inhibitor} \div C.R \text{ blank}) \quad (3)$$

3. Results and Discussion

3.1. Characterization of inhibitors

3.1.1. FTIR

The FTIR spectrum of the I-N-C8 compound is shown in Figure 2. This spectrum has bands at 533.65 cm^{-1} (C-I halo compound), 727.86 cm^{-1} (CH_2 aromatic), 1364.81 cm^{-1} (CH_2 aliphatic), 1058.45 cm^{-1} (N^+), and 1599.54 cm^{-1} (C=N). These bands conform to the expected function groups of the prepared compound [21]. found respectively. The two beaks at 230.12 and 118.41 are corresponding to ($\text{C}_7\text{H}_4\text{IN}^+$) and ($\text{C}_8\text{H}_{10}\text{N}_2^{++}$) respectively, which are formed in the case of breaking the bond between the two benzene rings.

3.1.2 Mass Spectroscopy

The mass spectrum of I-N-C8 is shown in figure 3. This spectrum indicates molecular ion peaks (M^+) at 543.29 which corresponded with the molecular formula ($\text{C}_{23}\text{H}_{32}\text{BrIN}_2$), at 543.33. The base peak at (349.09) may correspond to the molecular formula of alkyl chain break ($\text{C}_{15}\text{H}_{15}\text{IN}_2^{++}$). The two peaks at 77.10 and 127.14 suggested that (Br^+) and (I^+) ions are

found respectively. The two beaks at 230.12 and 118.41 are corresponding to ($\text{C}_7\text{H}_4\text{IN}^+$) and ($\text{C}_8\text{H}_{10}\text{N}_2^{++}$) respectively, which are formed in the case of breaking the bond between the two benzene rings.

3.1.3 Differential Scanning Calorimetry (DSC)

DSC is performed to investigate the mesosphere behaviour of the prepared compound. The values of enthalpy changes (J/g) at corresponding temperatures ($^\circ\text{C}$) show the phase transition of the I-N-C8 compound in cycles of heating and cooling, as shown in Table 2.

In the heating cycle, we observed two peaks at different temperatures with significant changes in enthalpy, with the lowest temperature corresponding to a small value of enthalpy, and vice versa. In the cooling cycle, we observed two peaks, with a high temperature corresponding to a high change in enthalpy. These results show that mesophase transition occurred during these conditions. Figure 4 shows two considerable changes during the heating process, the first peak at 128.32°C showing the beginning of the transition from crystal phase to mesophase, and the second peak at 158.40°C showing full isotropic deformation. However, the cooling cycle showed two considerable changes in temperature. The 143.06°C endothermic event showed that the isotropic/mesophase transition was occurred, and by lowering the temperature constantly, another endothermic change was spotted at 117.49°C , which expresses a full crystal form formation [22, 23]. These results showed that I-N-C8 compound reveals mesophase behavior which occurred because of the presence alkyl chain, which is flexible in nature and lined to the azomethane group in the structure [24].

3.2. Electrochemical Methods

3.2.1. Electrochemical Impedance Spectroscopy (EIS)

Table 3 shows impedance parameters such as charge-transfer resistance (R_{ct}), double-layer capacitance (C_{dl}), inhibition efficiency ($\eta\%$), and surface coverage (θ) of MS in 1 M HCl solution at 298 K with and without different concentrations of I-N-C8. Corresponding Nyquist plots and equivalent circuits proposed to fit impedance data are shown in Figure 5.

Table (1) shows a comparison between the prepared compound and many of already published related inhibitors for carbon steel in 1 M HCl.

Inhibitor name	Concentration	IE%	Ref
N-dodecyl-4-(((4-methoxyphenyl)imino)methyl)-N,N-dimethylbenzenaminium bromide	5 x 10 ⁻³ M	PP: 94.0,EIS:93.3	[38]
4-(((4-aminophenyl)imino)methyl)-N-dodecyl-N,N-dimethylbenzenaminium bromide		PP: 93.8,EIS:93.2	
N-dodecyl-4-(((4-hydroxyphenyl)imino)methyl)-N,N-dimethylbenzenaminium bromide		PP: 93.5,EIS:93.0	
4-(((4-chlorophenyl)imino)methyl)-N-dodecyl-N,N-dimethylbenzenaminium bromide		PP: 92.8,EIS:93.0	
N-dodecyl-N,N-dimethyl-4-(((4-nitrophenyl)imino)methyl)benzenaminium bromide		PP: 91.3,EIS:91.6	
2-(2-heptadecyl-2,5-dihydro-1H-imidazol-1-yl)ethan-1-ol	2 x 10 ⁻³ M	PP: 96.0,EIS:79.8	[40]*
(E)-N-hexadecyl-4-(((4-iodophenyl)imino)methyl)-N,N-dimethylbenzenaminium bromide	5 x 10 ⁻⁴ M	PP: 97.9,EIS:97.1	[39]
(E)-4-(((4-iodophenyl)imino)methyl)-N,N-dimethyl-N-octylbenzenaminium bromide	5 x 10 ⁻⁴ M	PP: 96.5,EIS:96.1	This study

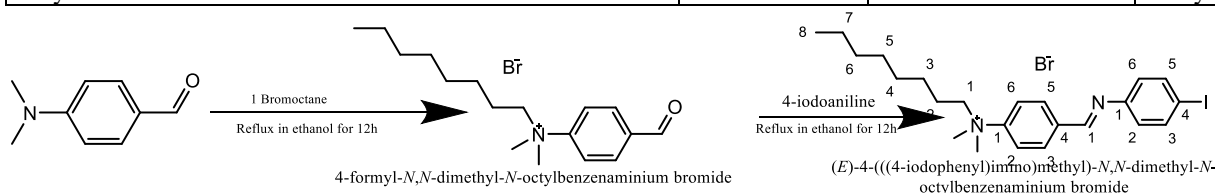


Figure 1: Preparation of inhibitor.

Table 2. Phase transition of I-N-C8 compound.

Cycle	T (°C)	ΔH(J/g)
DSC (cooling)	117.49°C	11.30J/g
	143.06°C	44.92J/g
DSC (heating)	158.40°C	69.91J/g
	128.32°C	1.399J/g

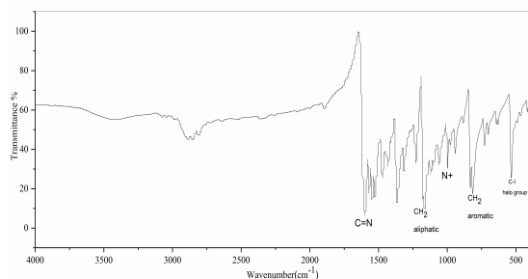


Figure 2. FTIR spectra of the prepared I-N-C8

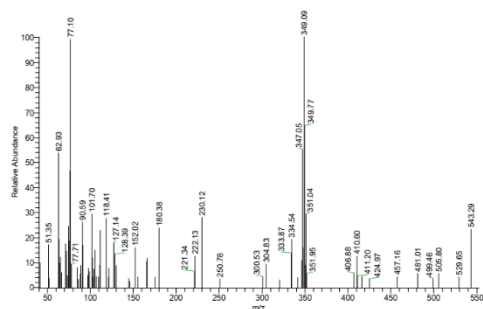


Figure 3. Mass spectra for compound I-N-C8.

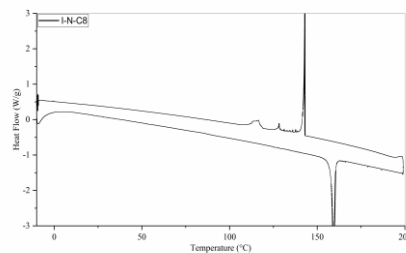
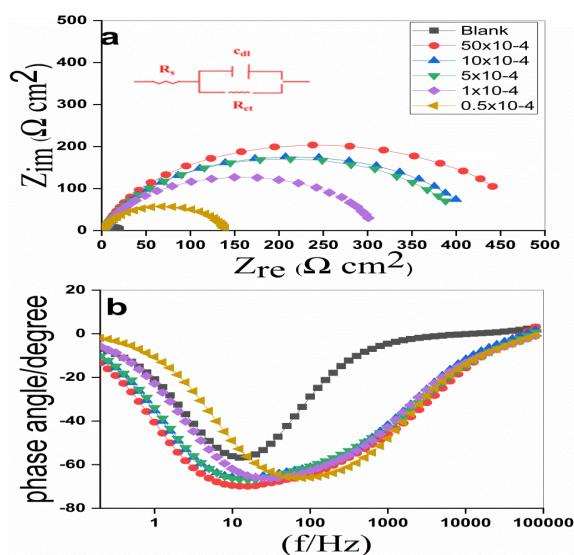


Figure 4. DSC of I-N-C8 compound.



The Chi-square values (around 10^{-3}) are teeny, indicating that the fitted data has a high degree of accuracy and minor error. The unaffected shape of the impedance curves shows that the same mechanism of MS dissolution occurs when I-N-C8 compound is added, but the addition of I-N-C8 compound at any concentration let to increase in the capacitive loop diameters, which refer to an increase in the inhibition of the corrosion. The results of EIS tests show that increasing the concentration of I-N-C8 compound has a direct proportionate effect on corrosion inhibition [25]. This is attributed to I-N-C8 molecules which have been adsorbed on the surface of the MS, obstructing active corrosion sites. The increase in Rct values can be explained by the progressive displacement of water molecules by I-N-C8 molecules adsorbed on metal surface, to form a barrier film which retards the corrosion in comparison to blank solution. This explained that I-N-C8 molecules were adsorbed on metal surface, leading to a decrease in rate of corrosion[26].

3.2.2. Potentiodynamic Polarization Technique

Table 4 shows the values of anodic Tafel (β_a), cathodic slopes (β_c), corrosion current density (I_{corr}), polarization resistance (Rp), surface coverage (θ), corrosion rate (C.R) and inhibition efficiency (η_p %)

of MS samples in 1 M HCl in absence and presence of different concentrations of the prepared inhibitor. It is clear from this data that the concentration of the I-N-C8 inhibitor is related to previous parameters. Polarization curves; a current versus potential (i vs. E) curve are shown in Figure 6. The concentrations of the inhibitor varied from 50 to 0.5×10^{-5} M. Figure 6 and Table 3 show that when the concentration of the inhibitor increases, the corrosion current (I_{corr}) in the acidic medium decreases, showing that this molecule has inhibitory properties.

The calculated η_p % results showed that, the greatest inhibition efficiency (96.19 %) which corresponds to the lowest (I_{corr}) value of ($46.100 \mu A cm^{-2}$) was observed at the highest added concentration (50×10^{-5} M at 298 K). Additionally, the corrosion rate (C.R) value at this concentration is 21.040 mpy, which is much lower than that obtained for MS corroded in blank sample (554.4 mpy) [27]. Generally, the potential increases with the concentration of the inhibitor added to the medium. Additionally, the anodic (a) and cathodic (c) Tafel constants changed significantly. From above results, the I-N-C8 compound showed high efficacy in controlling corrosion in an acidic medium, suggesting that it can be a promising material for supporting mild-steel surfaces in the face of corrosion attack[28]

Table 3.The EIS of MS in 1 M HCl with and without various concentrations of I-N-C8 compound at 298 K

Inhibitor	Conc (M)	Rs (Ru) (Ωcm^2)	Rct (Rp) (Ωcm^2)	Cdl ($\mu F cm^{-2}$)	Yo ($\mu \Omega^{-1} sn cm^{-2}$) $\times 10^3$	n	chi squared $\times 10^3$	θ	η_z %
Blank	----- -	1.038	18.87	3.39	4.477	0.899	0.352	-----	-----
I-N-C8	50×10^{-5}	0.874	551.6	0.20	0.562	0.806	5.854	0.9658	96.58
	10×10^{-5}	1.354	480.2	0.25	0.480	0.805	2.814	0.9607	96.07
	5×10^{-5}	1.240	469.7	0.37	0.545	0.785	5.540	0.9598	95.98
	1×10^{-5}	1.442	332.4	0.42	0.406	0.806	2.948	0.9432	94.32
	0.5×10^{-5}	1.049	142.7	0.60	0.359	0.839	0.837	0.8678	86.78

Table4. Values of the polarization parameters for MS in 1M HCl with and without different concentrations of I-N-C8 compound at 298 K

Inhibitor	Conc (M)	-Ecorr mV vsSCE	I_{corr} ($\mu A cm^{-2}$)	β_a (mV dec ⁻¹)	β_c (mV dec ⁻¹)	RP (Ω)	CR (mpy)	θ	η_p %
Blank	-----	-340	1210	0.1214	0.1561	7.433	554.4	-----	-----
I-N-C8	50×10^{-5}	-363	46.100	0.0843	0.1318	6.158	21.040	0.962	96.190
	10×10^{-5}	-382	53.800	0.0866	0.1219	9.033	24.580	0.956	95.554
	5×10^{-5}	-394	70.900	0.1121	0.1158	5.183	32.390	0.941	94.140
	1×10^{-5}	-368	91.800	0.0950	0.1393	3.441	41.940	0.924	92.413
	0.5×10^{-5}	-427	319.000	0.1260	0.1757	27.63	145.600	0.736	73.636

Table 5. EFM results for mild-steel in 1.0 M HCl at 298 K in with and without different concentrations of I-N-C8 compound at 298 K.

Inhibitor	Conc (M)	i_{corr} ($\mu\text{A cm}^{-2}$)	β_a	β_a (mV dec^{-1})	β_c	β_c (mV dec^{-1})	CF-2	CF-3	k (mpy)	θ	HEF M %
Blank	0	1210	-	73.76	-	92.82	2.033	3.191	460	-	-
I-N-C8	50×10^{-5}	47.490	0.094	93.56	1.31E-01	130.5	1.780	3.614	21.700	0.953	95.28
	10×10^{-5}	50.470	0.075	75.05	8.55E-02	85.45	1.669	4.593	23.060	0.950	94.99
	5×10^{-5}	58.290	0.088	88.47	1.18E-01	118.3	1.686	2.140	26.640	0.942	94.21
	1×10^{-5}	79.080	0.092	92.19	9.66E-02	96.57	2.286	3.109	36.140	0.921	92.15
	0.5×10^{-5}	159.00	0.086	85.91	9.89E-02	98.92	2.028	3.207	72.650	0.842	84.21

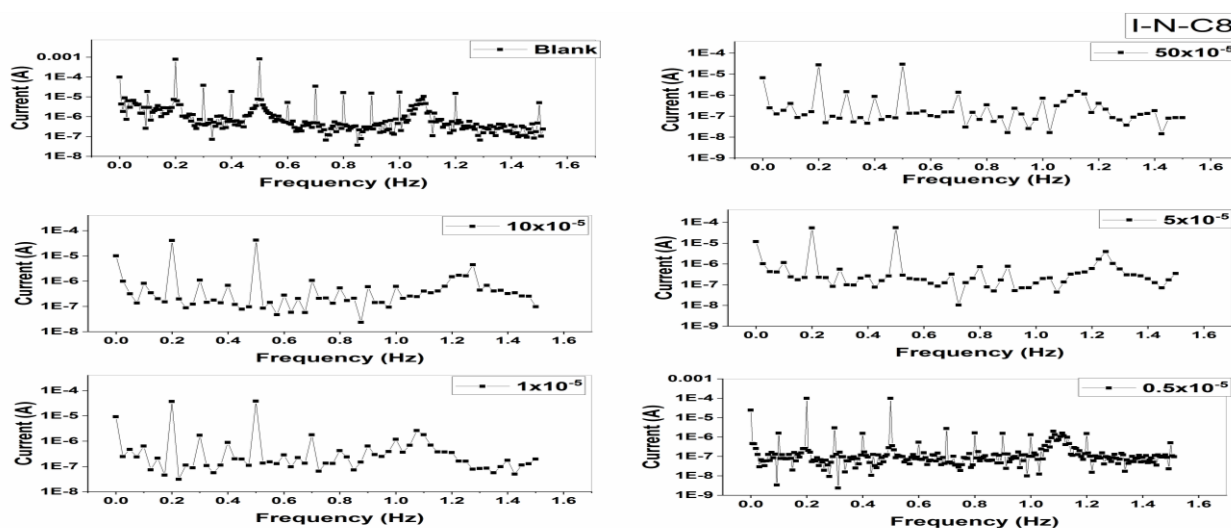


Figure 7. EFM spectra for MS in 1.0 M HCl with and without different concentrations of I-N-C8 compound at 298 K

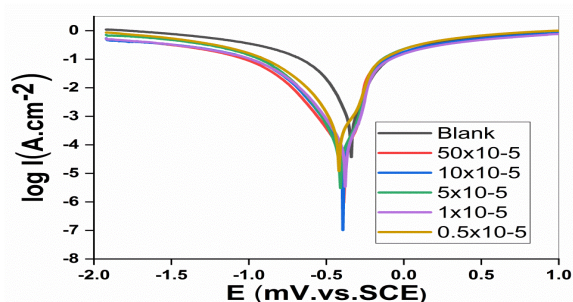


Figure 6. Polarization curves of MS in 1 M HCl with and without different concentrations of I-N-C8 compound

3.2.3. Electrochemical Frequency Modulation

Figure 7 and Table 5 show electrochemical parameters; corrosion current density (i) ($\mu\text{A/cm}^2$), Tafel constants (β_a , β_c), and causality factors (CF-2,

CF-3) are related to the concentration of the I-N-C8 compound. The corrosion inhibitor's efficiency was calculated as follows:

$$\eta_{\text{EFM}}\% = \left(1 - \frac{i_{\text{corr}}}{i^{\circ}_{\text{corr}}}\right) \times 100 \quad (4)$$

As [i_{corr}] is the corrosion current density at different concentrations of I-N-C8 and [i°_{corr}] is the corrosion current density without the I-N-C8 compound [29]; The values of the experimental factor values were found to be approximately equal to the theoretical values (2 and 3), showing that the data obtained was valid. From EFM results we can conclude that the addition of I-N-C8 to a 1 M HCl solution decreases the corrosion current densities, thus this compound can be considered as a good corrosion inhibitor in 1 M HCl for MS[30].

3.3. Non-electrochemical Methods

3.3.1. Weight loss Test

3.3.1.1. Concentration Factor

Weight loss, C.R, and IE% for MS samples exposed to 1 M HCl free and containing different concentrations of the I-N-C8 compound for 24 hours are shown in Table 5. The addition of I-N-C8 to the aggressive acidic solution reduced sample weight loss, C.R, and increased the IE% at all the selected concentrations of the inhibitor. The highest inhibition efficiency was obtained at the highest concentration of the inhibitor, and vice versa. This behavior is attributed to the strong interaction between the I-N-C8 compound and the metal's surface, which forms an isolation layer and thus minimize the surface area exposed to corrosive solution [31]. This interaction is enhanced by the inhibitor's aromatic structure (benzene ring and azomethane) and the donation of a lone pair of nitrogen heteroatoms in addition to the iodine atom [32, 33].

3.3.1.2 Temperature Factor

The corrosion of metals in acidic medium increases with temperature rise, which accelerates corrosion reactions. As expected, the corrosion rate of the blank sample increased by rising the temperature, Figure 8 and Table 5. In the case of the addition of the I-N-C8 compound, the corrosion rate increases with increasing temperature, however the IE % also increased. This may account for the ability of the I-N-C8 compound to be adsorbed on the metal surface under these conditions by chemisorption, forming coordinate bonds between pairs of electrons and empty orbitals of iron atoms [34]. Weight loss experiments performed at temperatures ranging from 298K to 338K show that the rate of adsorption is faster than the rate of desorption for the I-N-C8 compound on the mild-steel surface. Due to the fact that the equilibrium between adsorption and desorption processes on the metal surface is temperature dependent, we may expect that the adsorption process will greatly

accelerate before reaching a new equilibrium point. This increases the area covered by the I-N-C8 compound on the surface metal, hence increasing the inhibitory efficiency [35].

3.3.2 UV-visible Spectroscopy

The UV-visible absorption spectra of the 1M HCl solution containing 0.5×10^{-5} I-N-C8 before and after immersion of the MS for 24 h at room temperature is shown in Figure 9, the UV spectrum showed a maximum wave length of 195 nm, followed by a stable line up to 700 nm. However, after immersion for 24 h, the spectrum has a change in λ_{max} to 221 nm and the line has another peak at 456 nm, showing the presence of Fe^{2+} . However, the spectrum for the I-N-C8 compound before immersion shows a maximum absorption at 220 to 237 nm, then another λ_{max} at 361 which can be due to $\pi-\pi^*$ and $n-\pi^*$ transitions which the structure of I-N-C8 compound support that spectrum which have chromogen and auxochrome. After 24 h of immersion of MS in this medium, the high absorbance values changed from 220 to 242 and 318 to 378, showing the formation of a new complex between two species in solution. In these experiments, Fe^{2+} and I-N-C8 form a highly absorbent complex which results in an inhibitory effect [36].

3.4. Mechanism of Inhibitor Action

Adsorption is the principal process that supports corrosion inhibition. It is based on the inhibitor chemical structure "chemisorption," which contains (i) a nitrogen atom that shares electrons with the mild-steel surface; (ii) π -electron of aromatic ring in molecule interact with metal surface; (iii) a quaternary ammonium cation ($-N^+$) that has a positive charge, this part of the molecule tends to be absorbed on the positively charges on steel surface through negatively charged bromide ions [37]; (iv) the presence of iodo group as a donor group facilitates electron transfer from the azomethane group (C=N group) to the vacant d-orbitals of iron atoms on the surface of metal [38].

Table 6. Mass loss results for MS in 1M HCl with and without different concentrations of I-N-C8 compound at different temperatures

Conc inh (M)	298 ° K		308 ° K		318 ° K		328 ° K		338 ° K	
	CR x 10 ⁵	IE %	CR x 10 ⁵	IE %	CR x 10 ⁵	IE %	CR x 10 ⁵	IE %	CR x 10 ⁵	IE %
0	1.9821	-	4.5946	-	8.6916	-	69.6324	-	147.1686	-
50×10^{-5}	0.3732	81.85	0.6717	85.38	0.8459	90.27	3.9145	94.38	6.5933	95.52
10×10^{-5}	0.5722	72.18	1.1279	75.45	1.8245	79.01	10.7732	84.53	14.3560	90.25
5×10^{-5}	0.9288	54.84	1.6587	63.90	2.8280	67.46	18.2042	73.86	31.9134	78.32
1×10^{-5}	1.1445	44.35	2.3802	48.19	3.8730	55.44	23.8936	65.69	44.4118	69.82
0.5×10^{-5}	1.3352	35.08	2.7617	39.89	3.9145	54.96	28.7702	58.68	51.9174	64.72

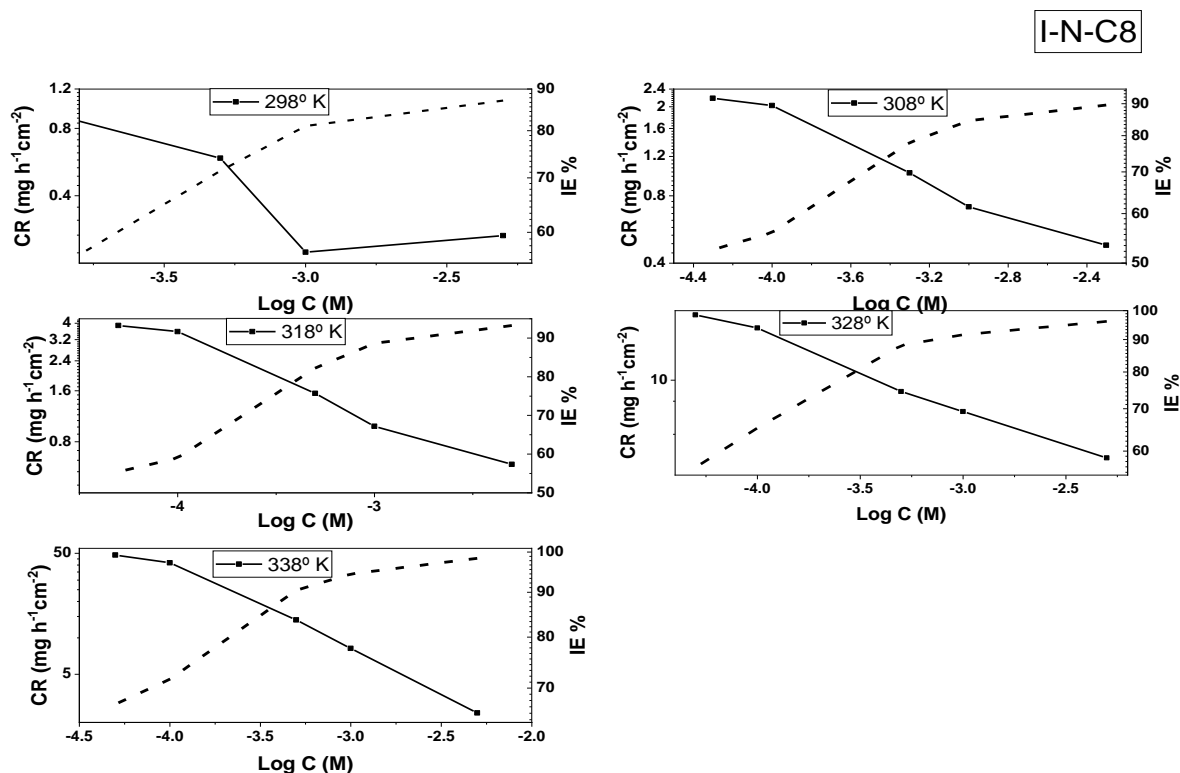


Figure 8. Corrosion rate (CR) and inhibition efficiency (IE %) relationship for MS in 1 M HCl with and without different concentrations of I-N-C8 compound at different temperatures

Concerning this research, the results obtained by using different techniques showed that the addition of the examined compound (LC, I-N-C8) significantly reduced the corrosion rate and highly affect the inhibition efficiency which reached about 97 %. This compound is designed so that its chemical structure supports the firm adsorption on the metal surface which reflected on the enhanced inhibition efficiency. In our previous article [39] the inhibition efficiency also reached about 97% by using a LC compound which was designed in the same way as I-N-C8 compound except that it contain longer hydrocarbon chain (16 carbon atoms) in comparison to 8 carbon atoms in case of I-N-C8 compound. This difference gives the prepared LC economic advantages over many similar compounds which have been published as corrosion inhibitors. This advantage arises from the stated results that the same or almost better inhibition efficiency can be achieved by using LC compounds include much shorter hydrocarbon chain which reflected positively on the preparation coast of the inhibitor for example 1-Bromooctane has lower cost than 1-Bromohexadecane and more available.

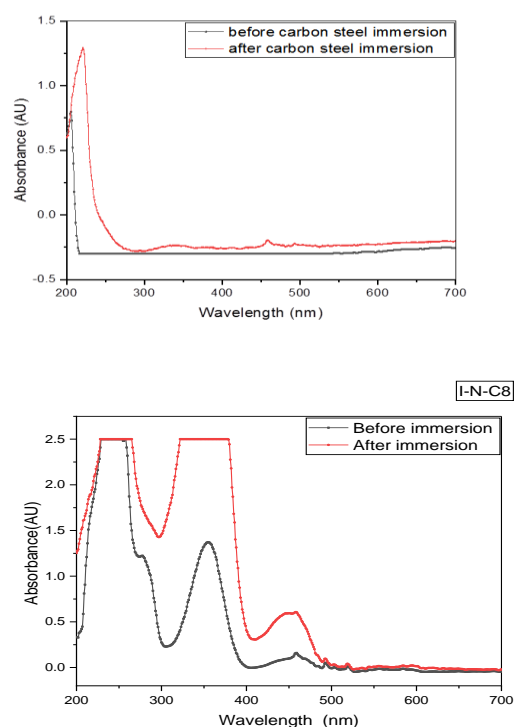


Figure 9. UV spectrum obtained from a 1 M HCl solution with (0.5×10^{-5}) I-N-C8 and without it before and after mild-steel immersion.

4. Conclusion

A new corrosion inhibitor compound designated I-N-C8 was successfully prepared and its chemical structure was approved by FTIR and mass spectrometry. The liquid crystal properties have been proved by using DSC method.

The corrosion inhibitor properties of the produced liquid crystal compound were evaluated for MS in 1 M HCl solution using electrochemical and non-electrochemical tests, which resulted in a perfect inhibition effect. According to electrochemical results, the I-N-C8 compound acts as mixed-type inhibitor that has been absorbed on the metal surface and covers the active sites on it. The rate of inhibition for the I-N-C8 compound increases as temperature rises because of liquid crystal properties, which generally support the stability of the suggested corrosion inhibitor in highly acidic conditions. The results of inhibition efficiency by different methods showed an enhanced effect. The presence of alkyl chain of only 8 carbon atoms didn't affect the inhibition efficiency as compared with the previously prepared LC of alkyl chain contains 16 carbon atoms which gives an economic advantage for the prepared new compound[39].

References

1. Abdallah M, Altass H, Al-Gorair AS, Al-Fahemi JH, Jahdaly B, Soliman K. Natural nutmeg oil as a green corrosion inhibitor for carbon steel in 1.0 M HCl solution: Chemical, electrochemical, and computational methods. *Journal of Molecular Liquids*. 2021;323:115036.
2. El Azhar M, Traisnel M, Mernari B, Gengembre L, Bentiss F, Lagrenee M. Electrochemical and XPS studies of 2, 5-bis (n-pyridyl)-1, 3, 4-thiadiazoles adsorption on mild steel in perchloric acid solution. *Applied surface science*. 2002;185:197-205.
3. James A, Oforka N, Abiola OK. Inhibition of acid corrosion of mild steel by pyridoxal and pyridoxol hydrochlorides. *International Journal of Electrochemical Science*. 2007;2:278-84.
4. <Nace-International-Report.pdf>.
5. Mostafa M. Khalefa , Hazem F. Khalil , S.T.Keera , Ashraf M. Ashmawy. Preparation and evaluation of Azo phenol as corrosion inhibitor for carbon steel in acid solution. *Egyptian Journal of Chemistry* 2022;65:791-802.
6. Deyab M, Ashmawy AM, Nessim M, Mohsen Q. New Gemini surfactants based on alkyl benzenaminium: Synthesis and links to application of corrosion protection. *Journal of Molecular Liquids*. 2021;332:115855.
7. Quraishi M, Rawat J. Inhibition of mild steel corrosion by some macrocyclic compounds in hot and concentrated hydrochloric acid. *Materials chemistry and physics*. 2002;73:118-22.
8. Loto RT, Loto CA, Joseph O, Olanrewaju G. Adsorption and corrosion inhibition properties of thiocarbanilide on the electrochemical behavior of high carbon steel in dilute acid solutions. *Results in Physics*. 2016;6:305-14.
9. Chakravarthy M, Mohana K. Adsorption and corrosion inhibition characteristics of some nicotinamide derivatives on mild steel in hydrochloric acid solution. *International Scholarly Research Notices*. 2014;2014.
10. Mostafa MA, Ashmawy AM, Reheim MAMA, Bedair MA, Abuelela AM. Molecular structure aspects and molecular reactivity of some triazole derivatives for corrosion inhibition of aluminum in 1 M HCl solution. *Journal of Molecular Structure*. 2021;1236.
11. Bassani F. *Encyclopedia of condensed matter physics*: Elsevier acad. press; 2005.
12. Okumus M, *Thermal properties of liquid crystal hexylbenzoic acid/octyloxybenzoic acid mixture*. 2015: Publisher.
13. Collings PJ, Goodby JW. *Introduction to liquid crystals: chemistry and physics*: Crc Press; 2019.
14. Ha S-T, Ong L-K, Sivasothy Y, Yeap G-Y, Lin H-C, Lee S-L, Boey P-L, Bonde NL. Mesogenic Schiff base esters with terminal chloro group: Synthesis, thermotropic properties and X-ray diffraction studies. *International Journal of Physical Sciences*. 2010;5:564-75.
15. Ha S-T, Lee T-L, Lee S-L, Sastry SS, Win Y-F. Schiff base liquid crystals with terminal iodo group: synthesis and thermotropic properties. *Scientific Research and Essays*. 2011;6:5025-35.
16. Ashmawy, A.M., Attia, S.K., Nessim, M.I., Elnaggar, E.S.M. and El-Bassoussi, A.A., Study on some azo liquid crystals as antioxidants for local base oil. *Molecular Crystals and Liquid Crystals*. 2018; 668:78-90.
17. Ashmawy AM, Nessim MI, Elnaggar EM, Osman DI. Preparation and evaluation of some novel liquid crystals as antioxidants. *Molecular Crystals and Liquid Crystals*. 2017;643:188-98.
18. Heakal FE-T, Elkholy AE. Gemini surfactants as corrosion inhibitors for carbon steel. *Journal of Molecular Liquids*. 2017;230:395-407.
19. Deghadi RG, Elsharkawy AE, Ashmawy AM, Mohamed GG. Can One Novel Series of Transition Metal Complexes of Oxy-dianiline Schiff Base Afford Advances in Both Biological Inorganic Chemistry and Materials Science? *Comments on Inorganic Chemistry*. 2021:1-46.
20. Bhadani A, Kataria H, Singh S. Synthesis, characterization and comparative evaluation of phenoxy ring containing long chain gemini imidazolium and pyridinium amphiphiles.

- Journal of colloid and interface science. 2011;361:33-41.
21. Ma H, Chen S, Yin B, Zhao S, Liu X. Impedance spectroscopic study of corrosion inhibition of copper by surfactants in the acidic solutions. *Corrosion Science*. 2003;45:867-82.
 22. Cesconeto RB, Rodrigues A, Dal-Bó AG, Dias NL, Rocha MRd, Frizon TEA. Evaluation of a thermochromic liquid crystal for use as a temperature sensor for components of electrical systems. *Materials Research*. 2017;20:130-6.
 23. Ashmawy AM, Elnaggar E-SM, Mohamed MG, Hamam MC. Preparation and evaluation of new liquid crystal compounds as flow improvers for waxy crude oil. *Journal of Dispersion Science and Technology*. 2020:1-15.
 24. Bhowmik PK, Chang A, Kim J, Dizon EJ, Principe RCG, Han H. Thermotropic Liquid-crystalline properties of viologens containing 4-n-alkylbenzenesulfonates. *Crystals*. 2019;9:77.
 25. Fateh A, Aliofkhaezai M, Rezvanian AR. Review of corrosive environments for copper and its corrosion inhibitors. *Arabian Journal of Chemistry*. 2020;13:481-544.
 26. Rajan DS, Malik SD. Surfactants as Corrosion Inhibitors for Stainless Steel in HCl Solution. *J Pure and Applied Science and Technology*. 2011;1:23-35.
 27. Barcia O, Mattos O, Pebere N, Tribollet B. Mass-transport study for the electrodisolution of copper in 1M hydrochloric acid solution by impedance. *Journal of the Electrochemical Society*. 1993;140:2825.
 28. Tadros T. Surfactants. In: Tadros T, editor. *Encyclopedia of Colloid and Interface Science*. Berlin, Heidelberg: Springer Berlin Heidelberg; 2013. p. 1242-90.
 29. Guo J, Zhang L, Liu S, Li B. Effects of hydrophilic groups of nonionic surfactants on the wettability of lignite surface: molecular dynamics simulation and experimental study. *Fuel*. 2018;231:449-57.
 30. Pal N, Saxena N, Mandal A. Studies on the physicochemical properties of synthesized tailor-made gemini surfactants for application in enhanced oil recovery. *Journal of Molecular Liquids*. 2018;258:211-24.
 31. Ashassi-Sorkhabi H, Asghari E, Ejbari P. Electrochemical studies of adsorption and inhibitive performance of basic yellow 28 dye on mild steel corrosion in acid solutions. *Acta Chim Slov*. 2011;58:270-7.
 32. Marzorati S, Verotta L, Trasatti SP. Green corrosion inhibitors from natural sources and biomass wastes. *Molecules*. 2019;24:48.
 33. Bedair M, Fouda A, Ismail M, Mostafa A. Inhibitive effect of bithiophene carbonitrile derivatives on carbon steel corrosion in 1 M HCl solution: experimental and theoretical approaches. *Ionics*. 2019;25:2913-33.
 34. Ismail KM, Elsherif RM, Badawy WA. Effect of Zn and Pb contents on the electrochemical behavior of brass alloys in chloride-free neutral sulfate solutions. *Electrochimica acta*. 2004;49:5151-60.
 35. Ramezanzadeh B, Arman S, Mehdipour M, Markhali B. Analysis of electrochemical noise (ECN) data in time and frequency domain for comparison corrosion inhibition of some azole compounds on Cu in 1.0 M H₂SO₄ solution. *Applied surface science*. 2014;289:129-40.
 36. El Achouri M, Kertit S, Gouttaya H, Nciri B, Bensouda Y, Perez L, Infante M, Elkacemi K. Corrosion inhibition of iron in 1 M HCl by some gemini surfactants in the series of alkanediyl- α , ω -bis-(dimethyl tetradecyl ammonium bromide). *Progress in Organic Coatings*. 2001;43:267-73.
 37. Brycki BE, Kowalczyk IH, Szulc A, Kaczerewska O, Pakiet M. Organic corrosion inhibitors. *Corrosion inhibitors, principles and recent applications*. 2018;3:33.
 38. Hegazy M, Ahmed H, El-Tabei A. Investigation of the inhibitive effect of p-substituted 4-(N, N, N-dimethyldodecylammonium bromide) benzylidene-benzene-2-yl-amine on corrosion of carbon steel pipelines in acidic medium. *Corrosion Science*. 2011;53:671-8.
 39. Ashmawy AM, El-Sawy AM, Khalil HF. Synthesis of novel liquid crystal compound and study of its behavior as corrosion inhibitor for mild steel in acidic medium (1 M) HCl. *Molecular Crystals and Liquid Crystals*. 2021:1-21.
 40. Jafari, H., Mohsenifar, F., & Sayin, K.. Effect of alkyl chain length on adsorption behavior and corrosion inhibition of imidazoline inhibitors. *Iranian Journal of Chemistry and Chemical Engineering (IJCCE)*. 2018, 37(5), 85-103.